A comparison between K and G approaches for a viscoelastic material: the case of environmental stress cracking of HDPE

Marco Contino*, Luca Andena, Vincenzo La Valle, Marta Rink
Dipartimento di Chimica, Materiali e Ingegneria Chimica "G.Natta", Politecnico di Milano, Piazza Leonardo da Vinci 32, 20133 Milano, Italy

Giuliano Marra, Stefano Resta
Fater S.p.A., R&D division, Via Ardeatina 100, 00071 Pomezia, Italy

*Corresponding author. Tel.: +390223993210;
E-mail address: marco.contino@polimi.it

Abstract

According to Linear Elastic Fracture Mechanics the stress intensity factor and the energy release rate are two fracture parameters linked by the elastic modulus and Poisson's ratio of the considered material. This concept has been extended to the analysis of linear viscoelastic materials, by introducing time-dependent quantities; it is also used for nonlinear viscoelastic polymers, even if its accuracy in this case is still an open question. In this work the Slow Crack Growth and the Environmental Stress Cracking resistance of two high-density polyethylene grades were investigated, differing for their molecular weight distribution and fracture resistance. The description of the fracture behaviour of the two materials provided by the stress intensity factor or the energy release rate turned out to be equivalent, despite the nonlinear mechanical behaviour exhibited by the two polymers. Moreover, a time-dependent effective modulus, related to the two fracture parameters, was evaluated: its value was in good agreement with the modulus experimentally determined from tensile tests. A constant relevant effective strain was found despite the different testing conditions (i.e. applied mechanical loading, temperature and presence of an active environment), its value being equal for the two considered polyethylenes.

Keywords

Fracture mechanics, pseudo-elastic approach, nonlinear mechanical behaviour, Slow Crack Growth, Environmental Stress Cracking, HDPE

1 Introduction

The stress intensity factor K describes the stress field around a crack within an elastic body; the energy release rate G in turn is the elastic energy change caused by an increase of the crack area. These two parameters, which have been at first defined within the Linear Elastic Fracture Mechanics (LEFM) theory, can be used to describe the fracture behaviour of many materials, providing a useful fracture criterion. As proved by (Irwin, 1957), according to the LEFM theory these two fracture parameters can be related following their two equivalent approaches; for plane strain conditions, the well known relationship holds:

$$G = \frac{K^2(1-\nu^2)}{E} \tag{1}$$

in which E and ν are the elastic modulus and Poisson's ratio of the considered material, respectively.

The stress intensity factor and the energy release rate are used as fracture parameters also within several viscoelastic theories, whose best-known examples are those proposed by Schapery (Schapery, 1975a, 1975b, 1975c) and by Williams and Marshall (Williams, 1972; Marshall and Williams, 1973; Williams and Marshall, 1975). Among these findings is that Equation (1) can be adapted, by introducing time dependent quantities, to describe the fracture behaviour of linear viscoelastic polymers.

This approximation, which constitutes the basis of the so-called pseudo-elastic approach, was found to be adequate to describe the behaviour of a variety of polymeric materials, among which were also some nonlinear viscoelastic materials. For instance, K and G were used for the analysis of the Slow Crack Growth (SCG) and Environmental Stress Cracking (ESC) of several polymers (Williams and Marshall, 1975; Frassine *et al.*, 1996; Kamaludin *et al.*, 2017), including:

- toughened polymethyl methacrylate (Mariani *et al.*, 1996; Pini *et al.*, 2018)
- high impact polystyrene (Andena *et al.*, 2013, 2016; Kamaludin *et al.*, 2016)
- polybutene (Andena *et al.*, 2009)
- polyethylene (Chan and Williams, 1983; Tonyali and Brown, 1986, 1987; Chang and Donovan, 1989; Rink *et al.*, 2003; Frank, Pinter and Lang, 2009; Contino *et al.*, 2016, 2018; Kamaludin *et al.*, 2016)

Assumptions on the validity of these two fracture parameters and of Equation (1) are supported by the accurate description of the fracture behaviour of the polymers considered in these works.

To further examine the validity of the pseudo-elastic approach, the SCG and ESC of two high-density polyethylenes, already studied in (Contino *et al.*, 2016, 2018) using the stress intensity factor approach and having a markedly nonlinear mechanical behaviour, were further analysed. Results in terms of G were compared with those obtained using the stress intensity factor. An effective modulus evaluated from these two quantities, according to Equation (1), was related to the material strain- and time-dependent modulus determined via tensile tests, to verify the equivalence of the two approaches.

2 Materials and methods

2.1 Experimental details

During this work, two blow moulding HDPE grades, supplied in pellets form by FATER S.p.A., were compression moulded into 1 mm and 11 mm thick plates, according to

the procedure described in (Contino *et al.*, 2018). These two materials have a monomodal and a bimodal molecular weight distribution and in the following will be named HDPE-MONO and HDPE-BI, respectively.

“Type 5 dumb-bell specimens” were obtained, via die cutting, from 1 mm thick plates according to ISO 527-3. Tensile tests were conducted on an Instron 1185R5800 electro-mechanical dynamometer equipped with a 10kN load cell at three temperatures (23, 40 and 60°C) and four displacement rates (1, 10, 50 and 100 mm/min). Specimen strain was measured optically: tests were videorecorded using a 10 MPixel µEye UI 5490 SE camera and the displacement of two markers, drawn on the sample gauge length, was evaluated using ImageJ software. At least two samples were tested at each temperature and strain rate condition and the obtained data were used to measure the time-dependent modulus of the two materials, as described in Section 2.2.2.

The 11 mm thick plates were machined, via circular saw cutting and milling, to obtain Single Edge Notched Bending (SENB) specimens having the geometry shown in Figure 1. A V-profile groove was introduced on both sides of the samples to guide crack propagation along the plane of the notch. The latter was made with an automated “chisel-wise” cutting machine to obtain a final notch root radius lower than 10 µm. SENB blunt notched samples were also prepared using a circular profile blade with 1 mm radius; these specimens were used to evaluate the crack initiation time and the propagation rate following a compliance calibration method.

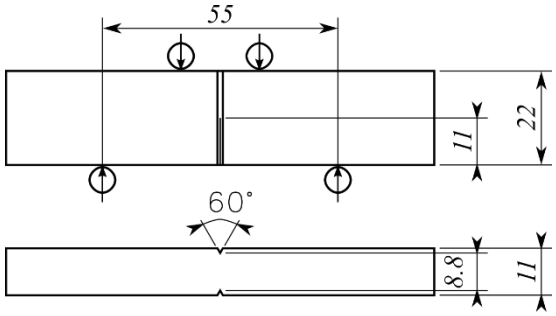

Figure 1 -Single Edge Notched Bending specimen geometry and nominal dimensions (in mm).

Fracture tests were conducted on a custom-built testing machine, in a four point bending configuration, applying a constant load to the specimens. The instrument, designed for tests at temperatures higher than room temperature, is composed by two fixed lower pins and two top ones, on which the load was applied by means of a pneumatic device, which releases a dead weight in a controlled way. Specimen deflection at the load pins was measured by a Linear Variable Displacement Transducer (LVDT). Tests were conducted at 40°C, 50°C and 60°C and at various constant loads.

Fracture tests were conducted both in air and, by placing the samples in flexible polyethylene bags, in the presence of two active environments having the following composition:

- Sol. A: an aqueous solution of sodium hypochlorite, sodium hydroxide, sodium carbonate, surfactants and perfume;
- Sol. B: a similar solution, in which sodium hypochlorite was replaced by an equal amount of water

Since, as already found in (Contino *et al.*, 2018), these two solutions have the same influence on the fracture resistance of the two HDPEs, no distinction between the two active environments will be made in the following.

2.2 Data analysis

2.2.1 Fracture behaviour

The fracture behaviour of the two materials was evaluated in terms of both crack initiation and propagation. To determine the crack initiation time and the crack growth rate a procedure based on the compliance calibration described in (Rink *et al.*, 2003; Andena *et al.*, 2013) was adopted. According to this method, the specimen compliance C can be expressed as

$$C = D(t) \cdot \Phi\left(\frac{a}{W}\right) \tag{2}$$

where $D(t)$ is the material creep compliance, $\Phi\left(\frac{a}{W}\right)$ is a known geometrical function which takes into account the presence of the notch in the sample, a is the crack length and W is the specimen width. For a blunt notched specimen the geometrical function is constant since crack initiation does not occur during the test; $D(t)$ can hence be determined for the material under study. Then, by measuring the compliance of a sharp notched specimen during a test, $\Phi\left(\frac{a}{W}\right)$ and then a can be easily evaluated. The continuous measurement of a during the test allows the direct determination of the crack initiation time and its subsequent growth rate. Because of significant data scatter due to irregular crack propagation, only an average value of crack speed was computed for each specimen within the range $0.5 < \frac{a}{W} < 0.6$.

Characteristic initiation and propagation curves were built by plotting both the crack initiation time and the crack growth rate vs. the stress intensity factor and the energy release rate, respectively. The fracture behaviour of the two materials in terms of the stress intensity factor K was already discussed in (Contino *et al.*, 2018) and only the main equations and results will be summarised in the following. The novelty of the current study is the analysis of the fracture behaviour of the two HDPEs in terms of the energy release rate G and the comparison of the two fracture approaches via the effective modulus E_{ef}, evaluated as reported in Sections 2.2.1.2 and 3, respectively.

2.2.1.1 Stress intensity factor

K was evaluated according to the following expression for SENB specimens in pure bending:

$$K = Y\frac{PS\sqrt{\pi a}}{B^* W^2} \tag{3}$$

where P is the applied load, S is the span length and W is the specimen width. The shape factor Y, valid up to $\frac{a}{W} = 0.6$, was computed as (Rooke and Cartwright, 1976):

$$Y = 1.12 - 1.39\left(\frac{a}{W}\right) + 7.32\left(\frac{a}{W}\right)^2 - 13.1\left(\frac{a}{W}\right)^3 + 14.0\left(\frac{a}{W}\right)^4 \tag{4}$$

An effective thickness, B^*, was considered in Equation 3 to take into account the effect of the side grooves on the stress distribution in the specimen ligament. In accordance with (Andena *et al.*, 2013), B^* was evaluated according to Equation 3:

$$B^* = B^{0.263} B_g^{0.737} \tag{5}$$

with B and B_g being the sample thickness of the ungrooved and grooved sections, respectively.

2.2.1.2 *Energy release rate*

The energy release rate G was evaluated starting from the equation proposed in (Williams, 1984):

$$G = \frac{U}{BW} \cdot \frac{1}{\psi\left(\frac{a}{W}\right)} = \frac{u \cdot P}{BW} \cdot \frac{1}{\psi\left(\frac{a}{W}\right)} \tag{6}$$

in which U is the energy stored in the specimen, u is the displacement measured by the LVDT and $\psi\left(\frac{a}{W}\right)$ is the calibration factor for the considered test configuration. The latter was evaluated, starting from the compliance C of the SENB specimen in four point bending, as:

$$\begin{gathered}\psi\left(\frac{a}{W}\right) = \frac{C}{dC/d\left(\frac{a}{W}\right)} = \\ \left\{\frac{15}{81} \cdot \frac{L^2}{W^2} + \frac{3}{8} \cdot (2+\nu) + \frac{2\pi L}{W}\left[0.6272\left(\frac{a}{W}\right)^2 - 1.0379\left(\frac{a}{W}\right)^3\right.\right. \\ +4.5822\left(\frac{a}{W}\right)^4 - 9.9387\left(\frac{a}{W}\right)^5 + 20.2267\left(\frac{a}{W}\right)^6 - 32.9577\left(\frac{a}{W}\right)^7 \\ \left.\left.+47.0713\left(\frac{a}{W}\right)^8 - 40.7556\left(\frac{a}{W}\right)^9 + 19.6\left(\frac{a}{W}\right)^{10}\right]\right\} \cdot \left\{\frac{2\pi L}{W}\left[1.2544\left(\frac{a}{W}\right)\right.\right. \\ -3.1136\left(\frac{a}{W}\right)^2 + 18.3289\left(\frac{a}{W}\right)^3 - 49.6936\left(\frac{a}{W}\right)^4 + 121.3604\left(\frac{a}{W}\right)^5 \\ \left.\left.-230.704\left(\frac{a}{W}\right)^6 + 376.57\left(\frac{a}{W}\right)^7 - 366.8\left(\frac{a}{W}\right)^8 + 196\left(\frac{a}{W}\right)^9\right]\right\}^{-1}\end{gathered} \tag{7}$$

2.2.2 Time-dependent modulus

The time-dependent modulus $E(t)$ of the two materials was evaluated from the engineering stress-strain ($\sigma - \varepsilon$) curves obtained from tensile tests at different displacement rates. The initial part of these curves was fitted with a two-term Prony series:

$$\sigma = \sigma_1 \cdot exp\left(\frac{\varepsilon}{\varepsilon_1}\right) + \sigma_2 \cdot exp\left(\frac{\varepsilon}{\varepsilon_2}\right) + \sigma_0 \tag{8}$$

where σ_0, σ_1, σ_2, ε_1, ε_2 are relevant fitting parameters. The fitting was performed to avoid excessive data scatter during the following numerical differentiation. $E(t)$ was evaluated at the three testing temperatures (23°C, 40°C and 60°C) and at various strain levels as the derivative of Equation (8):

$$\frac{d\sigma}{d\varepsilon} = E(t) = \frac{\sigma_1}{\varepsilon_1} \cdot exp\left(\frac{\varepsilon}{\varepsilon_1}\right) + \frac{\sigma_2}{\varepsilon_2} \cdot exp\left(\frac{\varepsilon}{\varepsilon_2}\right) \tag{9}$$

Time-temperature superposition was hence applied to extend the experimental window and to evaluate $E(t)$ also at the intermediate temperature of 50°C adopted during the fracture tests. The relevant master curves at the temperature of 60°C and at a few selected strain levels are shown in Figure *2* (a) and (b) for HDPE-MONO and HDPE-BI, respectively.

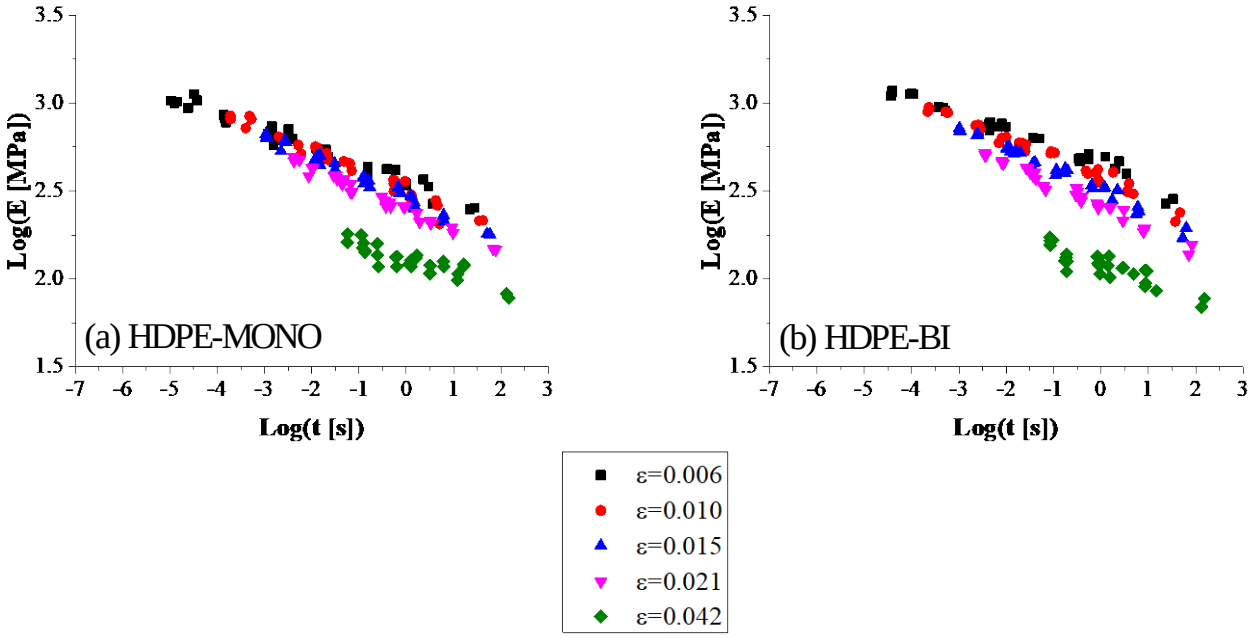

Figure 2 – Master curves of the time-dependent modulus at 60°C for a few selected strain values: (a) HDPE-MONO; (b) HDPE-BI.

3 Results and discussion

As shown in Figure 3 and Figure 4 (for initiation) and Figure 5 and Figure 6 (for propagation), the stress intensity factor K and the energy release rate G provide consistent trends, suggesting that, despite the nonlinear mechanical behaviour of the HDPEs considered in this work, the two fracture parameters can adequately describe their fracture behaviour. In the considered experimental range both K and G display a power law dependence on crack initiation time and propagation rate and by increasing the temperature the curves simply shift towards shorter initiation times and higher propagation rates. As expected from their different molecular weight distribution, HDPE-BI shows a considerably higher SCG resistance with respect to HDPE-MONO.

In presence of the active environment fracture is hastened: for a given value of K or G, crack is likely to initiate in a shorter time and then propagate at a higher rate. From the intersection of the air and environment branches, critical interaction times t_i^* and critical crack growth rates $\dot{a}^*$ were evaluated. These parameters, previously observed in (Chang and Donovan, 1990; Ward *et al.*, 1991; Ayyer, Hiltner and Baer, 2008; Andena *et al.*, 2013; Kamaludin *et al.*, 2017), reveal if a given environment will influence the fracture behaviour of a polymer. As a matter of fact, Environmental Stress Cracking will occur under conditions of K or G corresponding to fracture times that are longer than t_i^* and propagation rates lower than $\dot{a}^*$. In particular, for HDPE-MONO and HDPE-BI, it is possible to observe in Figure 7 that, for a given temperature, the critical interaction times and the critical crack growth rates evaluated using K or G are in good agreement, considering the data dispersion typically obtained in fracture tests. The critical interaction times and critical crack growth rates found for the two materials are very different, in accordance with HDPE-BI greater resistance to ESC. Nevertheless, as previously found in (Contino *et al.*, 2018), the same value of K^*, independent of the temperature and of the fracture phase, can be defined for both polymers who share the same molecular structure and a very similar degree of crystallinity, despite the difference in the molecular weight distribution. This similarity of the behaviour also holds

for G^*, evaluated in a similar way from energy release rate curves for initiation and propagation.

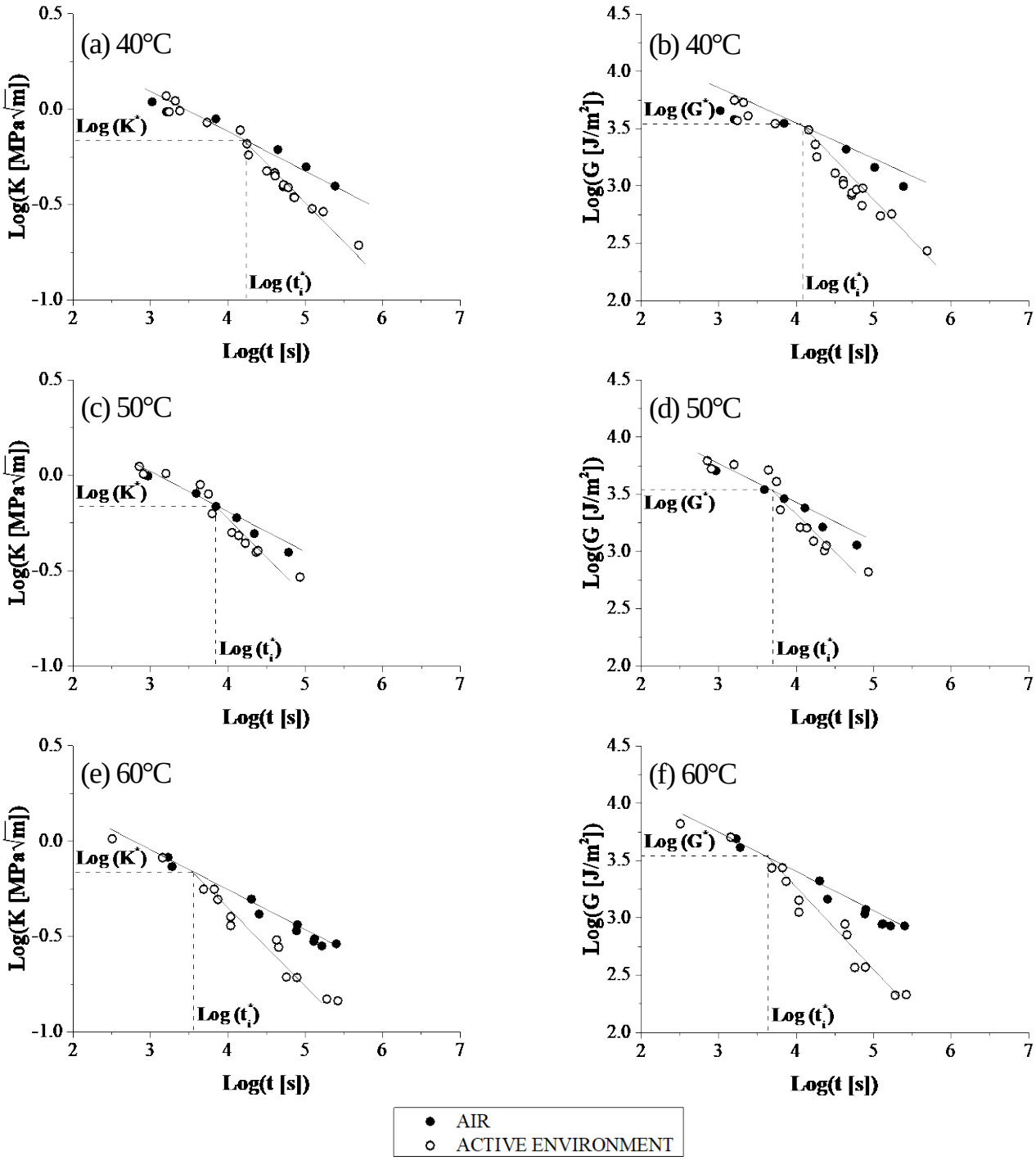

Figure 3 – Crack initiation behaviour of HDPE-MONO at different temperatures. (a,c,e) stress intensity factor vs. time at 40°C, 50°C and 60°C, respectively; these data were already reported in (Contino *et al.*, 2018). *(b,d,f) energy release rate vs. time at 40°C, 50°C and 60°C, respectively.*

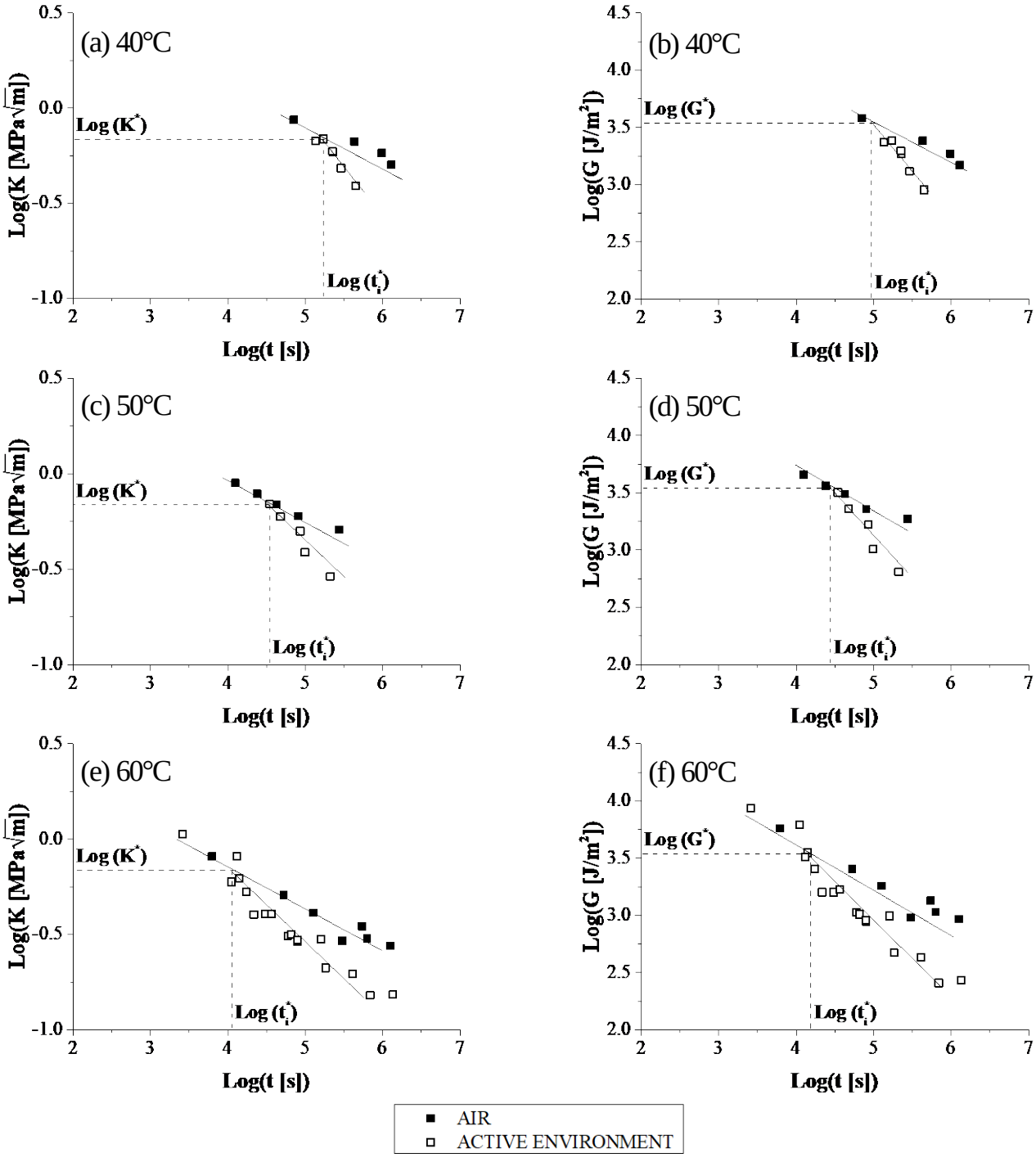

Figure 4 - Crack initiation behaviour of HDPE-BI at different temperatures.
(a,c,e) stress intensity factor vs. time at 40°C, 50°C and 60°C, respectively;
these data were already reported in (Contino *et al.*, 2018).
(b,d,f) energy release rate vs. time at 40°C, 50°C and 60°C, respectively.

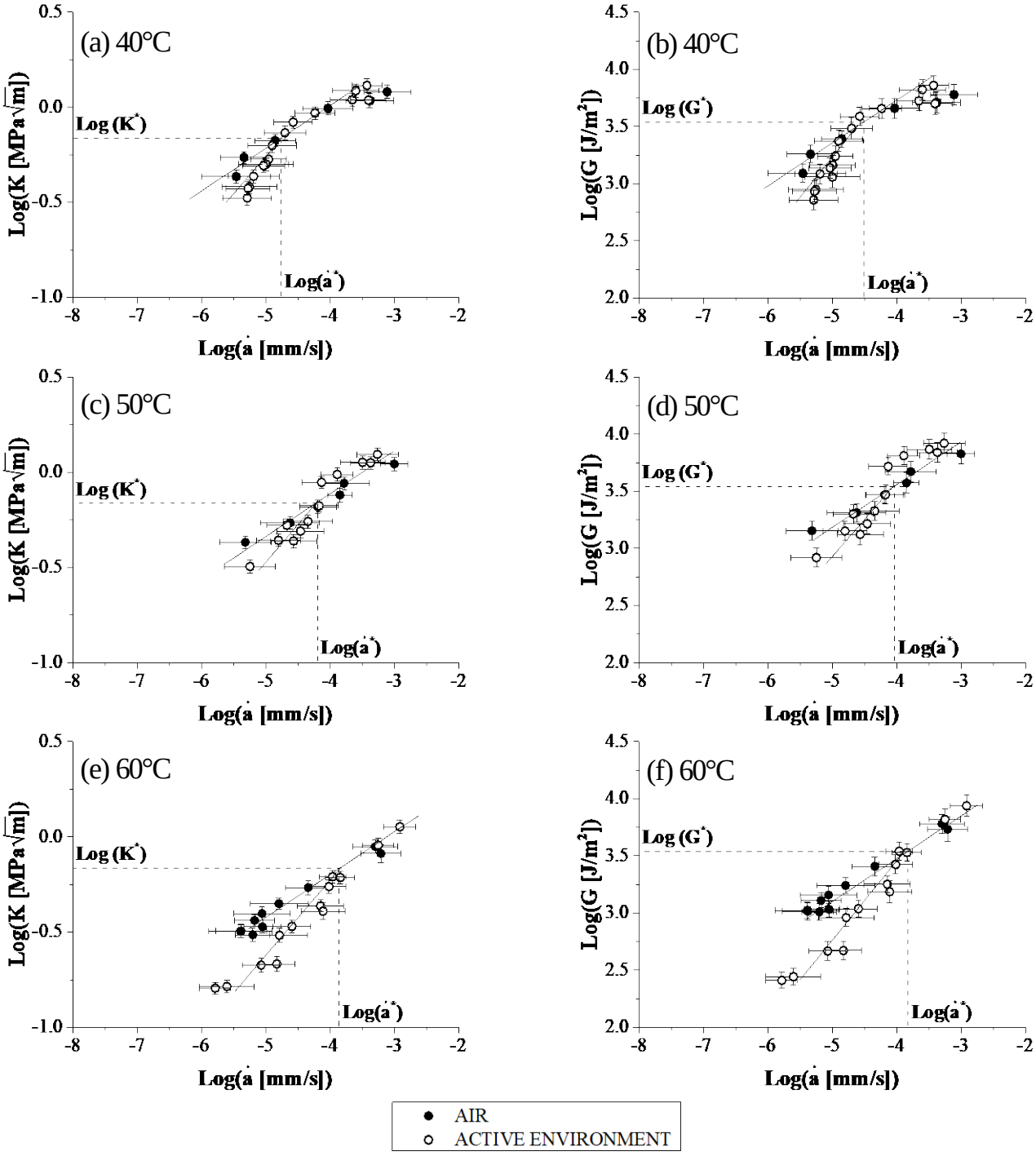

Figure 5 - Crack propagation behaviour of HDPE-MONO at different temperatures.
(a,c,e) stress intensity factor vs. crack growth rate at 40°C, 50°C and 60°C, respectively;
these data were already reported in (Contino *et al.*, 2018).
(b,d,f) energy release rate vs. crack growth rate at 40°C, 50°C and 60°C, respectively.

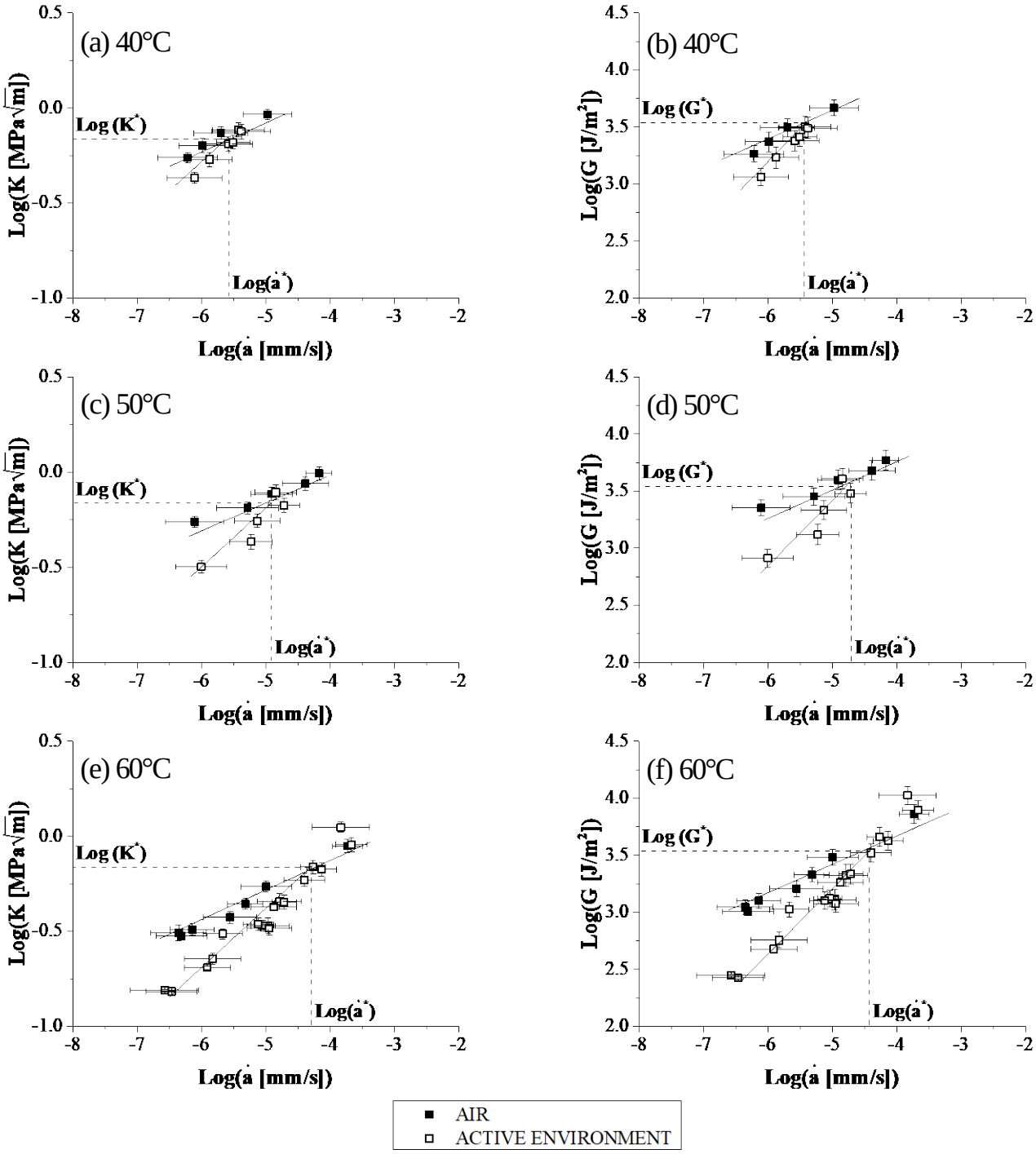

Figure 6 – Crack propagation behaviour of HDPE-BI at different temperatures.
(a,c,e) stress intensity factor vs. crack growth rate at 40°C, 50°C and 60°C, respectively;
these data were already reported in (Contino *et al.*, 2018).
(b,d,f) energy release rate vs. crack growth rate at 40°C, 50°C and 60°C, respectively.

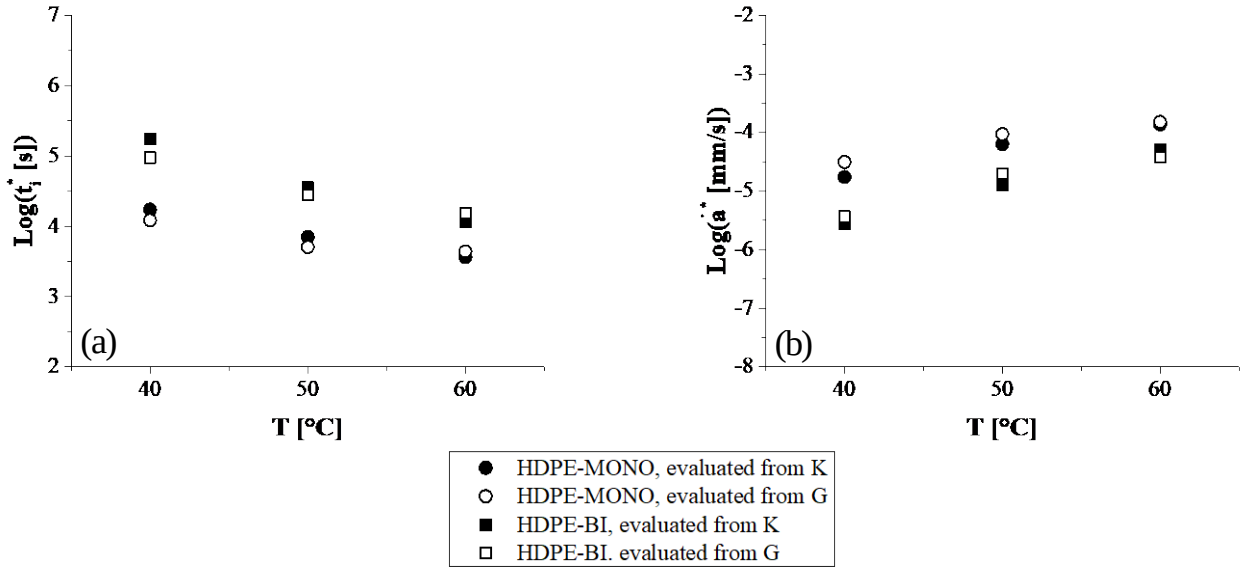

Figure 7 - Comparison between (a) critical interaction times and (b) critical crack growth rates evaluated using K or G as relevant fracture parameter.

To verify the validity of the pseudo-elastic approach also for the two nonlinear HDPEs under study, an effective modulus E_{ef} was evaluated, for both materials, as:

$$E_{ef}(t) = \frac{K^2(1-\nu^2)}{G} \tag{10}$$

where ν is the Poisson's ratio. Even if the time dependency of ν cannot be excluded, since would be between 0.3 and 0,5,variations of this property with time would yield only minor effects with respect to those caused by the time dependency of K and G; therefore, to simplify the analysis, during this study a constant value of 0.4 was assumed for ν. For each tested specimen, two pairs of K and G values were used to evaluate E_{ef}: one at the fracture initiation time, and one during crack growth, for which, in light of the limited range analysed ($\frac{a}{W} = 0.5 - 0.6$), an average time during propagation was considered.

Figure 8 reports, for all the considered temperatures and for both materials, the effective modulus vs. time curves (open symbols). At a single temperature, all data fall on the same curve irrespective of the fracture phase and of the presence of the active environment. Moreover, the E_{ef} curves at 40, 50 and 60°C seem to be simply horizontally shifted. These facts suggest that, probably, fracture occurs at a constant average strain level irrespective of the actual testing conditions and that the temperature and the active environment only alter the kinetics of this process.

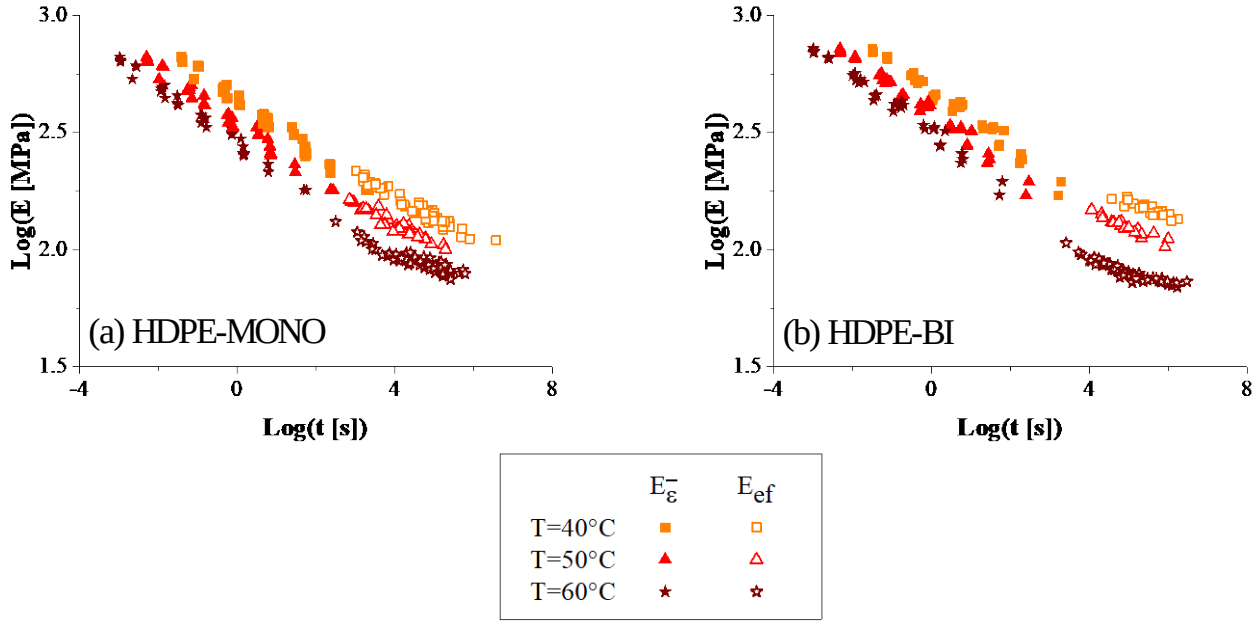

Figure 8 – Comparison between the time-dependent modulus at the average strain $\bar{\varepsilon} = 0.015$ and the effective modulus from fracture data. (a) HDPE-MONO; (b) HDPE-BI.

E_{ef} vs. t curve was then compared with a time-dependent modulus of the material at a relevant strain obtained with the procedure described in Section 2.2.2. To identify the relevant strain, an effective overall strain reached during the fracture process was evaluated. No direct measurement of the strain field in the specimen was available: an indirect estimation of this quantity was carried out applying the beam theory to the net (i.e. unnotched) ligament section. The maximum flexural strain in a beam under four point bending can be evaluated as:

$$\varepsilon = 4.70 \cdot u \cdot \frac{H}{S^2} \tag{11}$$

where H is the specimen width (taken equal to the ligament length, $W - a$), S is the span length and u is the measured mid-span displacement. This is an approximation since it assumes the maximum value of strain across the specimen cross-section but also neglects the intensification caused by the presence of the notch.

For each sample the strain at the boundaries of the considered propagation range was computed and expressed as a function of the relevant applied stress intensity factor, as shown in Figure 9. For both materials and at each temperature, the evaluated ε increases with increasing applied K and all the data fall on the same curve irrespective of the fracture phase (initiation or propagation) and of the presence of the active environment.

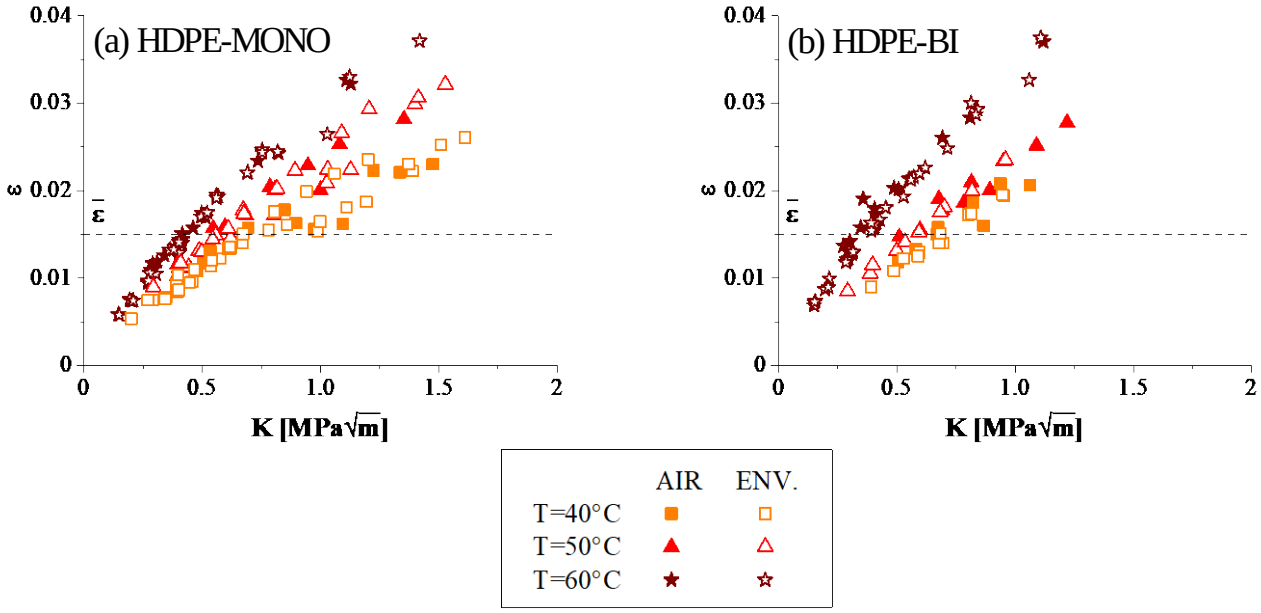

Figure 9 – Strains during the fracture tests evaluated as per Equation (11) as a function of the stress intensity factor. (a) HDPE-MONO; (b) HDPE-BI. $\bar{\varepsilon}$ is the average strain selected for the evaluation of the time-dependent modulus.

An intermediate level of strain $\bar{\varepsilon} = 0.015$, shown in Figure 9, was selected as the average of the values calculated for the different temperatures within the considered range of applied loading. The time-dependent modulus at this strain, as determined in section 2.2.2, is also reported in Figure 8.

It was found that, for both materials, the time-dependent modulus curves are in reasonable agreement with the effective modulus ones, confirming that the assumption of a fracture phenomenon occurring at an approximately constant strain is justified. The fact that fracture occurs at a critical strain which is similar for both polymers is somehow in agreement with the work reported in (Hiss *et al.*, 1999) where comparative studies on various polyethylenes led to the conclusion that their deformation behaviour under an applied tensile load has a common basis and is strain-controlled.

Since the effective modulus curves correspond to the time-dependent experimental ones at a constant strain level, the validity of the pseudo-elastic approach seems to apply also in the case of these nonlinear viscoelastic materials. Both the stress intensity factor and the energy release rate can be adopted to describe the fracture behaviour of the two considered HDPEs, and furthermore, if the average effective strain experienced during the fracture process is known, the relevant $E_{\bar{\varepsilon}}$ can be used in Equation (10) to evaluate G from K or vice versa.

4 Conclusions

During this work Slow Crack Growth and Environmental Stress Cracking of two nonlinear high-density polyethylenes tested at different temperatures were investigated by means of two approaches, based on the stress intensity factor and the energy release rate, respectively.

The description of the initiation and propagation behaviour of the materials following the two approaches seems equivalent: a power law dependence on the initiation time and the propagation rate was found and the effect of the temperature on the fracture kinetics was properly depicted. Both parameters were also able to represent the deleterious effect of the active environment on the material fracture resistance. The critical interaction times and crack growth rates evaluated following the two approaches were in fair agreement and, in both cases, a unique critical value of the considered fracture parameter, irrespective of the temperature and of the considered fracture phase, was found. For both environments considered (air and the active one), fracture resistance of the bimodal molecular weight distribution grade is larger – as expected. This influence of polymer chain length distribution (and thus entanglement density) indirectly confirms that SCG occurs according to the same mechanism irrespective of the environment, which only acts by accelerating fracture phenomena.

An effective modulus was evaluated from the stress intensity factor and the energy release rate: for both materials, the fracture process seems to occur at the same average strain for the different testing temperatures. This hypothesis was confirmed by the fair agreement between the effective modulus and the time-dependent modulus, obtained from tensile tests at the same average strain, irrespective of the applied stress intensity factor, fracture phase, temperature and the presence of the active environment. This fact implies that the relationship between the stress intensity factor and the energy release rate, defined within the Linear Elastic Fracture Mechanics framework, holds true also for the two nonlinear HDPEs considered in this work – provided a correct value for the time dependent modulus at the relevant overall strain is used.

5 Acknowledgements

The authors wish to thank Oscar Bressan (Politecnico di Milano) for helping with experiments and specimen preparation and Matteo Lega (FATER S.p.A.) for the preparation of the active solutions.

6 References

Andena, L. *et al.* (2009) ‘A fracture mechanics approach for the prediction of the failure time of polybutene pipes’, *Engineering Fracture Mechanics*, 76(18), pp. 2666–2677. doi: 10.1016/j.engfracmech.2009.10.002.

Andena, L. *et al.* (2013) ‘Determination of environmental stress cracking resistance of polymers: Effects of loading history and testing configuration’, *Engineering Fracture Mechanics*. Elsevier Ltd, 101, pp. 33–46. doi: 10.1016/j.engfracmech.2012.09.004.

Andena, L. *et al.* (2016) ‘Effect of processing on the environmental stress cracking resistance of high-impact polystyrene’, *Polymer Testing*. Elsevier Ltd, 54, pp. 40–47. doi: 10.1016/j.polymertesting.2016.06.017.

Ayyer, R., Hiltner, A. and Baer, E. (2008) ‘Effect of an environmental stress cracking agent on the mechanism of fatigue and creep in polyethylene’, *Journal of Materials Science*, 43(18), pp. 6238–6253. doi: 10.1007/s10853-008-2926-1.

Chan, M. K. V and Williams, J. G. (1983) ‘Slow stable crack growth in high density polyethylenes’, *Polymer*, 24(2), pp. 234–244. doi: 10.1016/0032-3861(83)90139-8.

Chang, P. and Donovan, J. A. (1989) ‘Crack size independence of the crack driving force in the buckled plate specimen’, *Journal of Materials Science*, pp. 816–820. doi: 10.1007/BF01148762.

Chang, P. and Donovan, J. A. (1990) ‘Detergent assisted stress cracking in low density polyethylene’, *Polymer Engineering & Science*, 30(22), pp. 1431–1441.

Contino, M. *et al.* (2016) ‘Fracture of high-density polyethylene used for bleach bottles’, *Procedia Structural Integrity*, 2(June), pp. 213–220. doi: 10.1016/j.prostr.2016.06.028.

Contino, M. *et al.* (2018) ‘Time-temperature equivalence in environmental stress cracking of high-density polyethylene’, *Engineering Fracture Mechanics*. Elsevier, 203, pp. 32–43. doi: 10.1016/j.engfracmech.2018.04.034.

Frank, A., Pinter, G. and Lang, R. W. (2009) ‘Prediction of the remaining lifetime of polyethylene pipes after up to 30 years in use’, *Polymer Testing*. Elsevier Ltd, 28(7), pp. 737–745. doi: 10.1016/j.polymertesting.2009.06.004.

Frassine, R. *et al.* (1996) ‘Experimental analysis of viscoelastic criteria for crack initiation and growth in polymers’, *International Journal of Fracture*, 81(1), pp. 55–75. doi: 10.1007/BF00020755.

Hiss, R. *et al.* (1999) ‘Network Stretching , Slip Processes , and Fragmentation of Crystallites during Uniaxial Drawing of Polyethylene and Related Copolymers . A Comparative Study’, *Macromolecules*, 32, pp. 4390–4403.

Irwin, G. R. (1957) ‘Analysis of Stresses and Strains near the End of a Crack Traversing a Plate’, *Journal of Applied Mechanics-Transactions of the ASME*, E24, pp. 351–369.

Kamaludin, M. A. *et al.* (2016) ‘Fracture mechanics testing for environmental stress cracking in thermoplastics’, *Procedia Structural Integrity*. Elsevier B.V., 2, pp. 227–234. doi: 10.1016/j.prostr.2016.06.030.

Kamaludin, M. A. *et al.* (2017) ‘A fracture mechanics approach to characterising the environmental stress cracking behaviour of thermoplastics’, *Theoretical and Applied Fracture Mechanics*. Elsevier Ltd, 92, pp. 373–380. doi: 10.1016/j.tafmec.2017.06.005.

Mariani, P. *et al.* (1996) ‘Viscoelasticity of Rubber-Toughened Poly(Methyl Methacrylate). Part II: Fracture Behavior’, *Polymer Engineering & Science*, 3(22), pp. 2758–2764.

Marshall, G. P. and Williams, J. G. (1973) ‘The correlation of fracture data for PMMA’, *Journal of Materials Science*, 8, pp. 138–140. doi: 10.1007/BF00755593.

Pini, T. *et al.* (2018) ‘Fracture toughness of acrylic resins: Viscoelastic effects and deformation mechanisms’, *Polymer Engineering & Science*, 58(3), pp. 369–376. doi: 10.1002/pen.24583.

Rink, M. *et al.* (2003) ‘Effects of detergent on crack initiation and propagation in polyethylenes’, in Blackman, B. R. K., Pavan, A., and Williams, J. G. (eds) *Fracture of Polymers, Composites and Adhesives II*. Elsevier, pp. 103–114. doi: 10.1016/S1566-1369(03)80087-0.

Rooke, D. P. and Cartwright, D. J. (1976) *Compendium of stress intensity factors*. Edited by T. H. Press. Uxbridge (Middlesex,U.K.).

Schapery, R. A. (1975a) ‘A theory of crack initiation and growth in viscoelastic media I. Theoretical development’, *International Journal of Fracture*, 11(1), pp. 141–159. doi: 10.1007/BF00034721.

Schapery, R. A. (1975b) ‘A theory of crack initiation and growth in viscoelastic media II. Approximate methods of analysis’, *International Journal of Fracture*, 11(3), pp. 369–388. doi: 10.1016/s0378-5173(98)00068-4.

Schapery, R. A. (1975c) ‘A theory of crack initiation and growth in viscoelastic media III. Analysis of continuous growth’, *International Journal of Fracture*, 11(4), pp. 549–562. doi: 10.1007/BF00116363.

Tonyali, K. and Brown, H. R. (1986) ‘On the applicability of linear elastic fracture mechanics to environmental stress cracking of low-density polyethylene’, *Journal of Materials Science*, 21(9), pp. 3116–3124. doi: Doi 10.1007/Bf00553345.

Tonyali, K. and Brown, H. R. (1987) ‘Effects of detergent concentration and ethylene oxide chain length of the detergent molecule on stress-cracking of low-density polyethylene’, *Journal of Materials Science*, 22(9), pp. 3287–3292. doi: 10.1007/BF01161193.

Ward, A. L. *et al.* (1991) ‘The mechanism of slow crack growth in polyethylene by an environmental stress cracking agent’, *Polymer*, 32(12), pp. 2172–2178. doi: 10.1016/0032-3861(91)90043-I.

Williams, J. G. (1972) ‘Visco-elastic and thermal effects on crack growth in PMMA’, *International Journal of Fracture Mechanics*, 8(4), pp. 393–401. doi: 10.1007/BF00191101.

Williams, J. G. (1984) *Fracture mechanics of polymers*. Chichester: Limited, Ellis Horwood.

Williams, J. G. and Marshall, G. P. (1975) ‘Environmental Crack and Craze Growth Phenomena in Polymers’, *Proceedings of the Royal Society of London. Series A, Mathematical and Physical Sciences*, 342(1628), pp. 55–77.